WORLD CONFERENCE ON TIMBER ENGINEERING 2025
BRISBANE, AUSTRALIA
Advancing Timber for the Future Built Environment

60-MINUTE COMBUSTION TEST UNDER LOADING OF STEEL BAR-TIMBER COMPOSITE BEAMS

Shinichi Shioya [1] and Shizuka Matsushita[2]

ABSTRACT: Recently, timber buildings are desired from a viewpoint of global warming, and moreover, in severe earthquake prone zones, such as Japan, they are more desired on the grounds of light weight of timber members. We are developing a frame system formed by hybrid timber members strengthened with deformed steel bars (i.e. rebars) using epoxy resin adhesive. To practice the system, it is necessary to investigate fire resistance performance of the members. As a trial, we conducted a 60-minute burn test of one relatively small cross section of a steel bar-timber composite beam and reported its results in previous WCTE 2023. Now, for practical use, we have conducted a 60-minute combustion test of three beams with relatively large cross sections. This paper reports the experiment and its results.

KEYWORDS: *Fire, Burning margin, Steel bar-timber composite beam, Deformed steel bar*

1 – INTRODUCTION

Nowadays cross laminated timber (CLT) is being used for buildings. However, CLT often restricts planning of buildings because it is flat plate members. To improve the flexibility of their planning, higher stiffness and strength are desired for column and beam. We have been developing a frame system formed with steel bar-timber composite members which can perform better than those of reinforced concrete structure [1]. As a trial, we conducted a 60-minute burning test of one steel bar-timber composite beam with a small cross section and reported its results in previous WCTE 2023[1]. Now, for practical use, we have conducted a 60-minute combustion test of three beams with relatively large cross sections and long spans.

2 – CONCEPT FOR STRENGTH CAPACITIY

Resisting area assumed in a beam section during its burning for 60-minutes is illustrated in Figure 1(a).

i) Basic concept is to divide the section into three segments in the width/210mm as shown Figure 1(b); the central segment is expected to resist as the composite beam because of being cooler than the allowable upper limit temperature of 70˚C for the composite beam. Uncharred wood portion and the central rebar are assumed to be able to resist at the allowable stress-level for short-term loading.

ii) Additional wood laminas to the extent of 90mm thickness are bonded to lower surface of the beam, as fireproof for lower rebar of the beam. The additional laminas are assumed not to expect its resisting in design.

3– COMBUTON TEST AS A TRAIAL REPORED AT THE PREVIOUS WCTE

We already conducted a 60-minute combustion test on a steel rebar-timber composite beam and reported on it at WCTE2023.

The specimen was only one, and it had double-array of rebar at upper and lower portions in its beam cross section. Its wood was Japanese cedar, and it was laminated using resorcinol adhesive. Maximum load for long-term loading in design was applied to the specimen and it was burned for 60-minutes. After then, the load

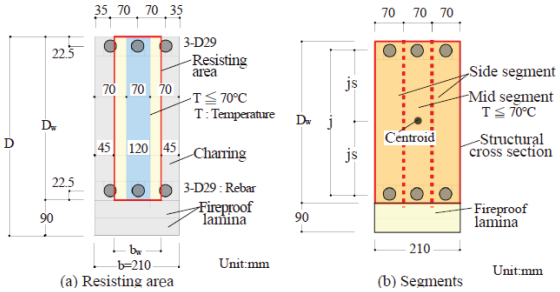

Figure 1: An expected cross-section after 60 - minute burning

[1] Shinichi Shioya, Department of Architecture, Kagoshima University, Kagoshima, Japan, k7347039@kadai.jp

[2] Shizuka Matsushita, Ishimoto Architectural Design Company, Tokyo, Japan, k3608908@kadai.jp

https://doi.org/10.52202/080513-0710

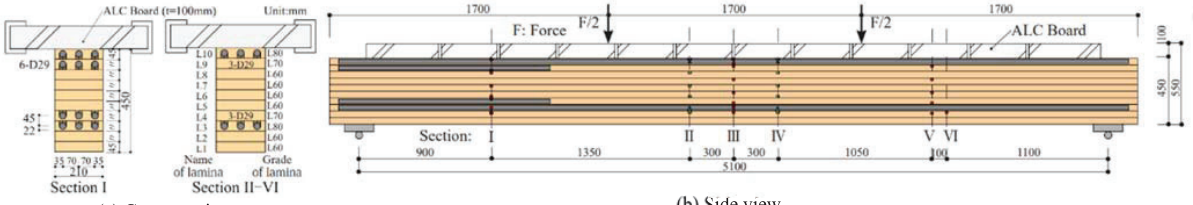

(a) Cross-section (b) Side view

Figure 2: Specimen

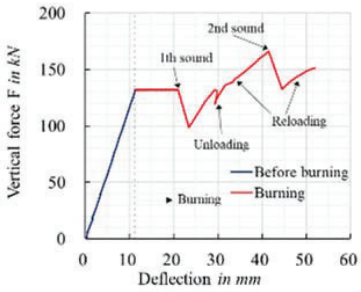

Figure 3: Force-deflection

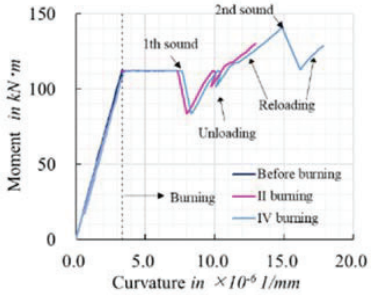

Figure 4: Moment-curvature

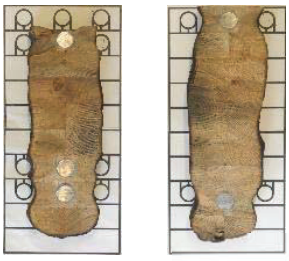

(a) *Section I* (b) *Section III*

Photo 1: Residual wood after test

(a) *Specimen immediately after burning test* (b) *Specimen cooled with water*

Photo 2: Specimen after combustion test

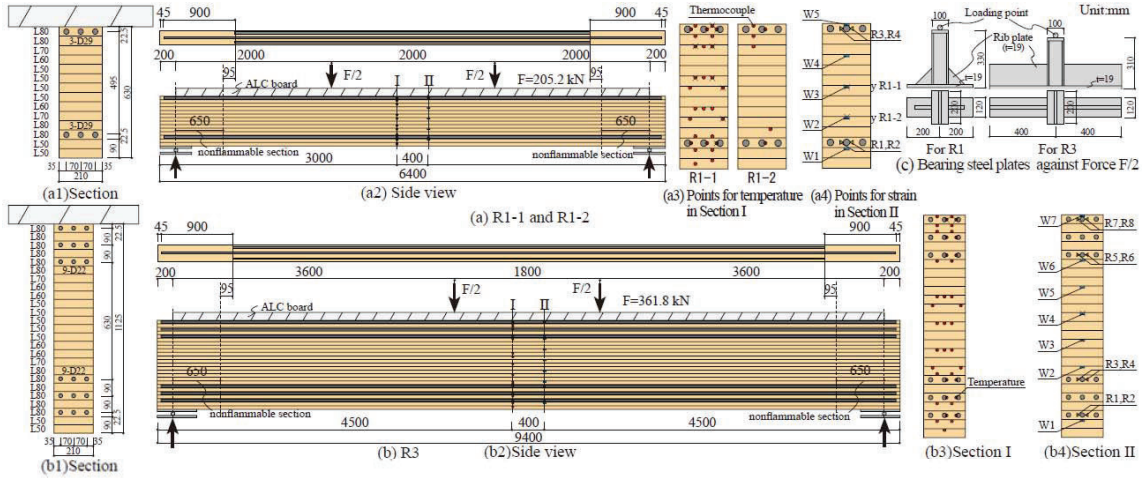

Figure 5: Cross sections and side views of specimens, locations of strain gauge, and thermocouple (Unit: mm*)*

was increased in the furnace used. Figure 3 shows force-deflection relationship; Figure 4, moment-curvature relationship; Photo 1, residual wood after combustion test; Photo 2, side views after combustion test. At 59 minutes-30 seconds and 63 minutes-33 seconds, an impact sound occurred, and the load decreased due to buckling of upper compression rebar in beam. At this, the loading was stopped. This 60-minute of combustion confirmed that the strength capacity calculated from the approach to exclude the burning margin in Figure 1(a) and the limitation value for deflection in the semi-fireproof of criteria of beam (1/30 of the span length) were satisfied. After that, combustion was stopped. after 6 months passed, the specimen was transported to Kagoshima-university and loaded at room temperature to investigate its maximum strength capacity, please, refer to Reference 1.

4 –COMBUSTION TEST FOR 60-MINUTE SEMI-FIREPROOF CERTIFICATION

4.1 SPECIMEN

https://doi.org/10.52202/080513-0710

Table 1: Mechanical properties of lamina

Grade of lamina	Bending test					Tensile test				
	Pure lamnina			Finger joint		Pure lamnina			Finger joint	
	n	E	σ_m	n	σ_m	n	E	σ_m	n	σ_m
L80	5	10369	80.9	3	53.1	3	6267	45.5	3	31.5
L70	3	8639	62.6	2	38.0	3	8897	39.1	2	15.9
L60	5	8947	57.1	—	—	3	5950	26.7	—	—
L50	3	5634	50.2	2	25.4	3	5546	34.8	2	19.6

n: The number of testpieces
E :Young's modulus
σ_m : Strength

Table 2: Moisture content in %

Specimen	L50	L60	L70	L80	Average
R1-1	9.61	10.34	9.70	10.13	9.94
R1-2	10.74	10.93	10.15	9.68	10.37
R3	9.73	10.21	9.99	10.82	10.19

Table 3: Mechanical properties of rebar

Rebar	E	σ_y	σ_{tu}
D22	1.89×10^5	460	653
D29	1.90×10^5	441	629

E :Young's modulus
σ_y :Yielding strength
σ_{tu} :Tensile breaking strength

Table 4: Assumed values and results for calculation for bending moment strength/M_u and shear strength/Q_{wfsu} after combustion test

Specimen	D_w	b_w	F_w	F_r	F_{wb}	f_{wbs}	kz	A_w	y_t,y_c	I_{wo}	I_w	Z_w	M_{wu}	a_{ro}	f_{ry}	j	M_{ry}	M_u	L_s	M_u/L_s	F/2 →	F	Q	f_{wss}	κ_{sf}	Q_{wfss}	Q/Q_{wfss}
	in mm		*in* N/mm²					*in* mm²	*in* mm	*x10⁶ in* mm⁴	*x10⁶ in* mm⁴	*in* mm³	*in* kN m	*in* mm²	*in* N/mm²	*in* mm	*in* kNm		*in* m		*in* kN		*in* kN	*in* N/mm²		*in* kN	
R1	540	120	6500	2.05×10^5	22.5	15.0	0.93	2333	270	1.6	1.3	4.8	66.6	642	390	495	124	191	2.0	95.3	102.6 →	205.2	102.6	1.8	1.26	92.4	1.11
R3	1035						0.85	1475	518	11.1	9.6	18.5	234.8	387		810	367	602	3.6	167.1	180.9 →	361.8	180.9		1.37	163.2	1.11

$I_{wo}=b_w D_w^3/12$, $I_w=I_{wo}\sum 2A_w(j_i/2)^2$, $Z_w=I_w/(D_w/2)$, $M_{wu}=k_z Z_w f_{wbs}$, $M_{ry}=a_t f_{ry} j$, $M_u=M_{wu}+M_{ry}$, $F/2=1.08\,M_u/L_s$, $Q=F/2$, $Q_{wfss}=f_{wss} b_w D_w/\kappa_{sf}$
D_w, b_w, j_s, j: See Fig.1., A_w: Sum of area of one rebar and invalid area of wood around rebars, a_s, a_c: area per one rebar,
k_z: Size factor for bending strength of timber, y_t, y_c : Height from centroid to upper fringe and lower fringe orver

Table 5: Assumed values and results calculated for bending moment strength/Mu and shear strength before burning test

Specimen	D_w	b	M	M_{ry}	a_t	A_w	F_{wb}	f_{fy}	Z_{wo}	M_{wu}	M_u	M/M_u	σ_{wb}	σ_t	Q	κ_s	τ_m	f_{wsL}	τ_m/f_{wsL}
	in mm		*in* kN m		*in* mm²		*in* N/mm²		*x10⁶ in* mm³	*in* kN m			*in* N/mm²		*in* kN		*in* N/mm²		
R1	540	210	205	372	1927	1170	22.5	390	8.61	180	552	0.37	5.6	161	102.6	1.26	1.14	0.99	1.15
R3	1035		651	1101	1161	766			32.98	627	1728	0.38	6.1	183	180.9	1.37	1.14		1.15

$M=Q\,L_s$, $M_{ry}=a_t f_{ry} j$
$I_{wo}=b\,D_w^3/12 - 2\Sigma 3\,A_w y_i^2$
$Z_{wo}=I_{wo}/y_t$, $M_{wu}=k_z Z_{wo} F_{wb}$
$\tau_m=\kappa_s\,Q/(b\,Dw)$
b: See Fig.1.

Figure 5 illustrates configuration of specimens. In the performance evaluation for semi-fireproof, it was necessary to determine the range of application of the calculation method for strength capacity, and structural cross-section in design was assumed to have a beam width of 210-240mm and a beam depth of 540-1035mm, with a rebar diameter of D22-D29. Taking account of adverse conditions for heating, including the safety factor of the loading weight, two cross-sections was selected. For the performance certification, two specimens are required for one same cross-section. For that, a cross section with one array of rebars was selected. Furthermore, to confirm that a beam with depth of 1035mm, multi-layer array of rebars, and a rebar diameter of D22 could be applied, a cross-section with a structural cross-section dimension of 210x1035mm and D22 three-stage reinforcement was selected, and its specimen was manufactured to be one. Figure 5(a1) and Figure 5(b1) show the cross-section of specimen and the grade of laminas. The former is the cross-section of one-layer array of rebar and the latter is that of triple-layer array. The former is two specimens of the same size, and the latter is one specimen. The former is named as R1 and the latter is done as R3. As R1 has two specimens, they each are distinguished as R1-1 and R1-2. Figure 5(a2) and Figure 5(b2) show side views and views from above, respectively. The ends of side rebar were cut off in the heating section for the following reasons. As shown in Photo 1(a), the side rebar was observed, after the combustion test, to be bent. The support portions on the left and right of the specimen are covered so that they would not heat up, and this can prevent the bent rebar from falling. If the ends of side rebars were cut off in the heated section, there was a concern that they would fall and heating around the side rebar would penetrate deeper, reducing the strength capacity.

Figure 5(a3) and Figure 5(b3) show the locations of thermocouples in cross-section I. Figure 5(a4) and Figure 5(b4) show the locations of foil strain gauges in cross-section II. The locations of the cross sections within the specimens are shown in Figure 5(a2) and Figure 5(b2). In cross section I, internal temperatures were measured, and in cross section II, strains of wood and rebar were measured. W means strain of wood and R means strain of rebar. Due to connection mistake between their lead wires, it was not possible to measure all the strain gauges and thermocouples. These are indicated by X in the figures.

Table 1 shows mechanical properties of laminas used in specimens. Table 2 shows moisture contents of the laminas. Table 3 shows mechanical properties of rebars. Diameter of rebar for R1 is D29, and that for R3 is D22, and its material grade is SD390. The shape of the rebars was a threaded rebar, for the ease of joining the members to each other[3]. Process of gluing a rebar into lamina and shape of U-groove and wooden cover were improved to reduce the labor required for manufacturing timber for the composite beam.

4.2 LOADING AND MEASUREMENT

Loading employed four-point bending; lengths of pure bending section and shear span section, and diameter of rebar were selected so that bending moment at the centre of the span and shear force at the shear span on both sides would be slightly greater than the bending

https://doi.org/10.52202/080513-0710

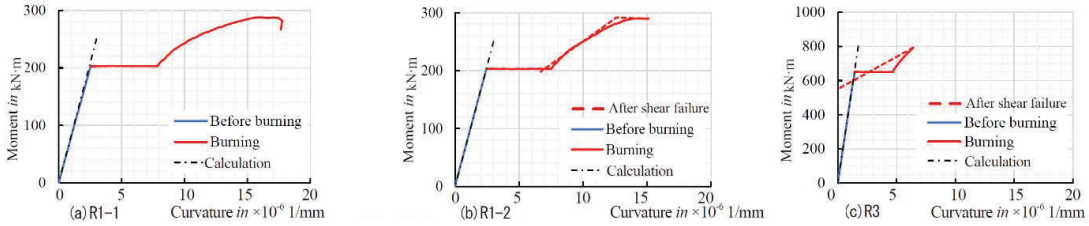

Figure 6: Bending moment - curvature relationship

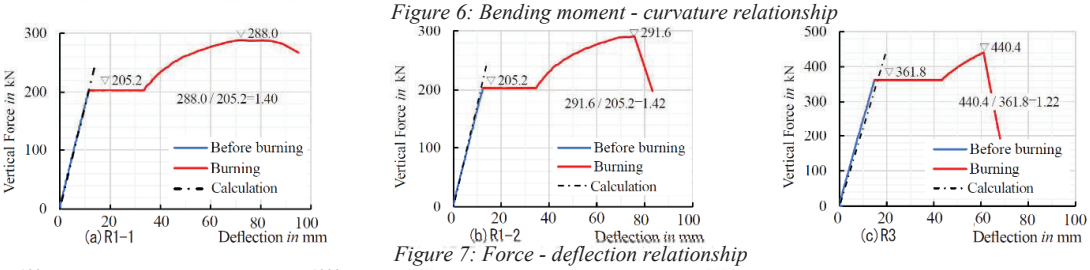

Figure 7: Force - deflection relationship

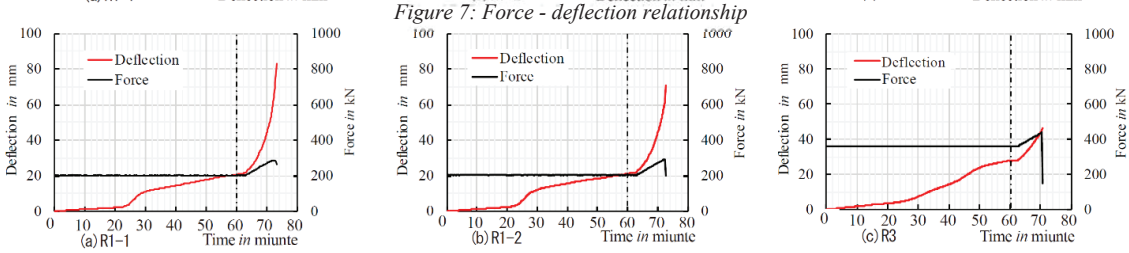

Figure 8: Deflection of mid-span and Force/F during burning test

and shear resistance calculated based on the uncharred portion expected within the cross-sections at 60-minute burning. To prevent lateral buckling of the beam, the loading plate of the loading point in Figure 5(c)was screwed to the specimens, and the T-shaped part welded to the loading plate (upper right of Photo 3(a)) was restrained laterally to prevent buckling. On the base of the approach in Chapter 2, the flexural and shear strength capacities of the uncharred cross-section were calculated. Table 4 shows the values calculated. The additional lamias were ignored in the calculation. The loading force/ F was assumed to be 205.2 kN for R1 and 361.8 kN for R3. To estimate, in design, strength capacities on the safe side, F was set to a value approximately 8% larger than that at the calculation of the flexural capacity M_u. The shear force Q during loading exceeded the short-term allowable shear force Q_{wfsu} that could be supported by the uncharred portion within beam section by approximately 11% for both R1 and R3. If F can be supported in the heating test, the result will argue that the beam can withstand more than the short-term allowable shear force that can be supported by the remaining cross-section. Table 5 shows the calculations for the cross-section before heating. As a result, the loading force was set so that the bending moment due to loading slightly exceeded 1.1/3 (=36.7%) of the bending strength. However, stress of wood/σ_{wb} and stress of rebar/σ_r were both below long-term allowable stresses of timber (8.25 N/mm^2) and the long-term allowable stress of rebar (195 N/mm^2), respectively. The shear stress of timber exceeded the long-term allowable shear stress of timber by 15%.

4.3 COMBUSTION TEST

The combustion test was conducted in the furnace of a performance evaluation organization in Osaka Prefecture in Japan from February 9 to 15, 2023. Heating was started 15 minutes after loading was completed up to the targets, respectively. The heating was conducted according to the standard heating curve based on ISO 843-1. Heating was stopped at 60 minutes after heating; then the force was increased to collapse the specimen. Figure 6 shows moment-curvature relationship. Figure 7 shows vertical load-deflection relationship. The definitions of moment, curvature, load and deflection are the same as in Reference 2. Blue curve indicates relationship during applying load up to the target; red curve is the relationship after the start of heating. The relationship based on the calculated value of bending stiffness before heating is shown in Figure 6 as a black dotted line. The cross-sectional second moment of area is calculated using Young's modulus of

https://doi.org/10.52202/080513-0710

lamina in Table 6. Young's modulus of rebar is assumed to be the standard value ($2.05x10^5 N/mm^2$). The calculations estimated the stiffness of the experiments with an accuracy of 0.0 to +1.0% error. The validity of the assumption of the unity of strain between wood and steel rebar and the assumption of the plane section after bending was also confirmed in a cross-sectional dimension of 210 x 1035 mm with three layers of rebar. The calculated deflection stiffness is shown in Figure 7 as a black dotted line. The calculated stiffness was estimated with an accuracy of -5.5 to +3.0% error compared to the experiments.

4.4 DEFLECTION AND LOAD DURING HEATING

Change in deflection and load during heating is shown in Figure 8. The red curve shows change in deflection. For all three specimens, the deflection increases rapidly after 24 minutes. However, the increase in R3 is slower than that in R1. This is because R3 has a larger beam depth than R1, and, of R3, ratio of the depth of carbonization at the bottom of the beam to the initial beam depth is smaller, so the rate of decrease in deflection stiffness is smaller. The black curve indicates change in force/F in Figure 8. All three specimens were able to support the loading load set for 60 minutes of heating and satisfied the deflection limit (1/30 of the span length) required for the certification.

4.5 LOAD-DEFLECTION RELATIONSHIP AND FAILURES DUE TO ADDITIONAL LOADING TO COLLAPSE

Deflection and force increased in Figure 7 and Figure 8 because the load was boosted to cause collapse after heating for 60 minutes. As can be seen in Figure 7, R1-1 and R1-2 reached their yield strength capacity and then had a range where they maintained their strength capacity, but R3 did not have the range and dropped suddenly immediately after the maximum force peak. The initial target force, maximum load after the 60-minute heating, and the safety factor (ratio of maximum load to loading load) are shown in Figure 7. Photo 3 shows specimens removed from the furnace after combustion test. In R1-1, indentation was observed at a loading point, as seen in Photo 3(a), below the loading steel plate. This probably occurred after bending yield of beam. In R1-2, no indentation failure observed, and horizontal cracks occurred in beam web, as seen in Photo 3(b). Shear failure probably occurred after the flexural yielding of beam. In R3, an impact sound occurred during loading, and its force suddenly

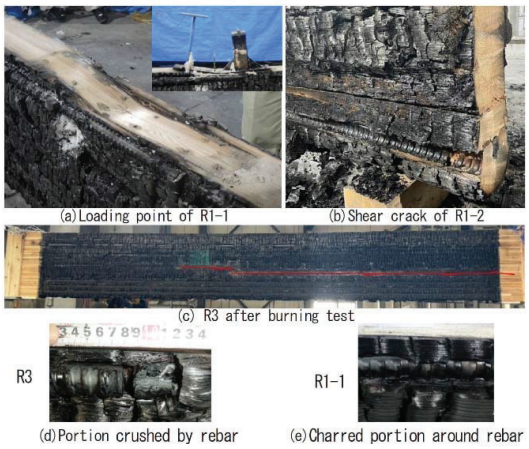

Photo 3: Specimen after combustion test

decreased. As shown in Photo 3(c), horizontal cracks (red line) occurred in the web. The reason that the indentation failure did not occur in R3 probably was that the bearing area of the loading plate in Figure 5(c) was larger in R3 than in R1. The side rebars did not bend in any of the specimens, as can be seen in Photo 3(c) against previous specimen in Photo 2. As seen in Photo 3(d), the ends of the side rebars extended axially and the charred portions were scraped off. As seen in Photo 3(e), the side rebars were caught by the charred portion in all of specimens, and this probably is why they did not fall off after 60 minutes of burning. However, several bars fell just before the maximum load while increasing the load after 60-minutes of heating.

4.6 STRAIN DURING BURNING

In the moment-curvature relationship shown in Figure 6, R1-1 shows an increase in curvature at a constant moment after reaching maximum moment. R1-2 and R3 show a rapid reversal of curvature immediately after the maximum moment. After the reversal, the red dotted line is shown. This is due to the shear failure causing beam cross-section to shift horizontally and therefore the strain in wood to decrease. Figure 9 shows changes of strains of the wood and the central rebar. The horizontal axis is time from the start of heating. Red broken curve and dotted curve are the rebar, broken curve is the single-array rebar, and the dotted curve at R3 is the third array rebar. Yield strain of the rebar is shown by black horizontal dotted line. Temperature rise in the central rebar was approximately 8℃ even at the end of the loading test. The yield strain of the rebar was increased by the temperature-induced strain ($+80\mu$). In the calculation, linear expansion coefficient of the rebar was assumed to be $1.0x10^{-5}$/℃. At 60-minute, the

https://doi.org/10.52202/080513-0710

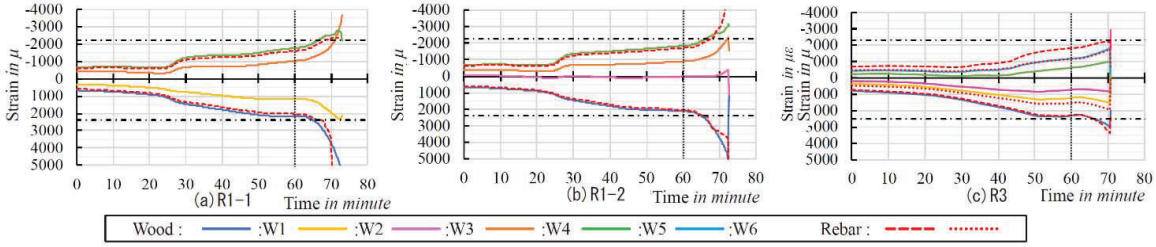

Figure 9: Strains of wood and rebar in Section II

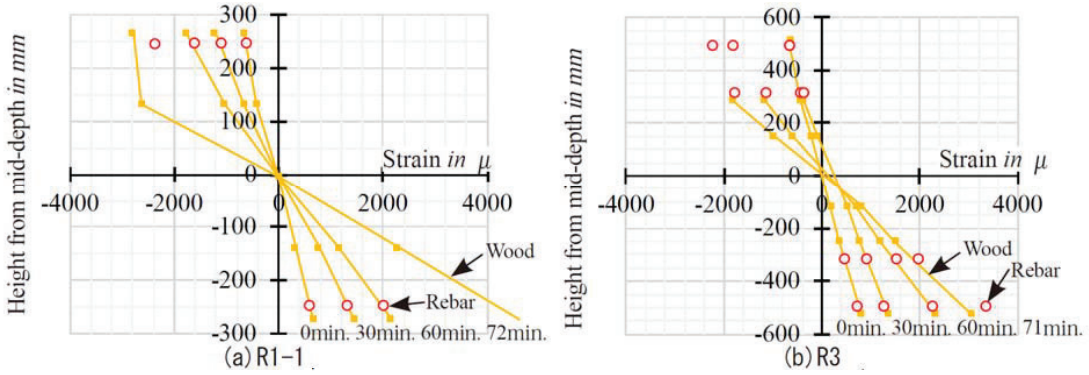

Figure 10: Bending strain profiles during

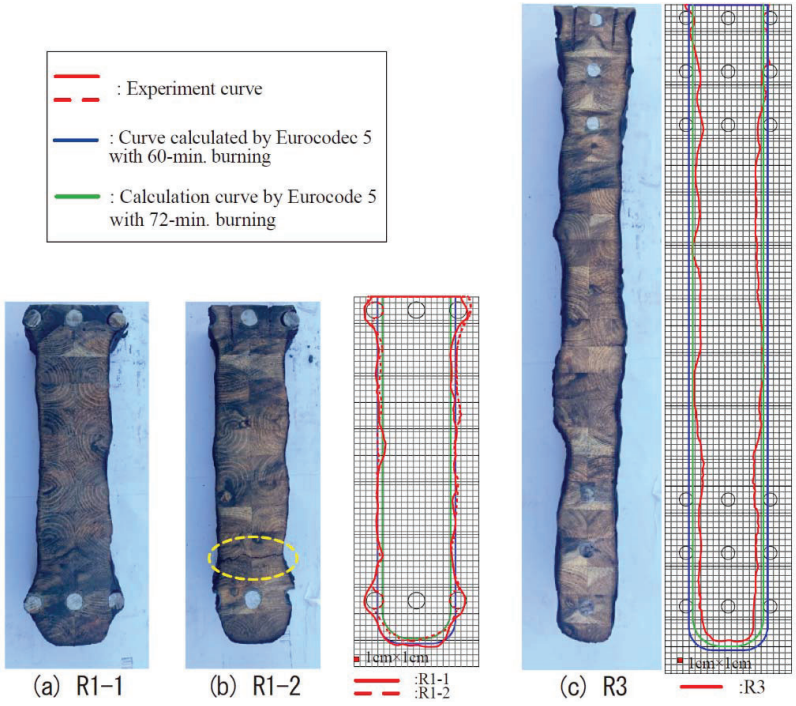

Photo 4: Cross-sections after 1-hour burning test

strain(red broken curve) of the first-array rebar from an upper or lower surfaces of beam of the specimens approached the yield strain of rebar, but they had not yet yielded. However, R1 yielded when subjected to further additional. R1 failed in bending; R1-1 in indentation fracture at the loading point; R1-2 in shear fracture. In R3, the first-layer array rebars reached the yield strain just before reached maximum load, but there was no

https://doi.org/10.52202/080513-0710

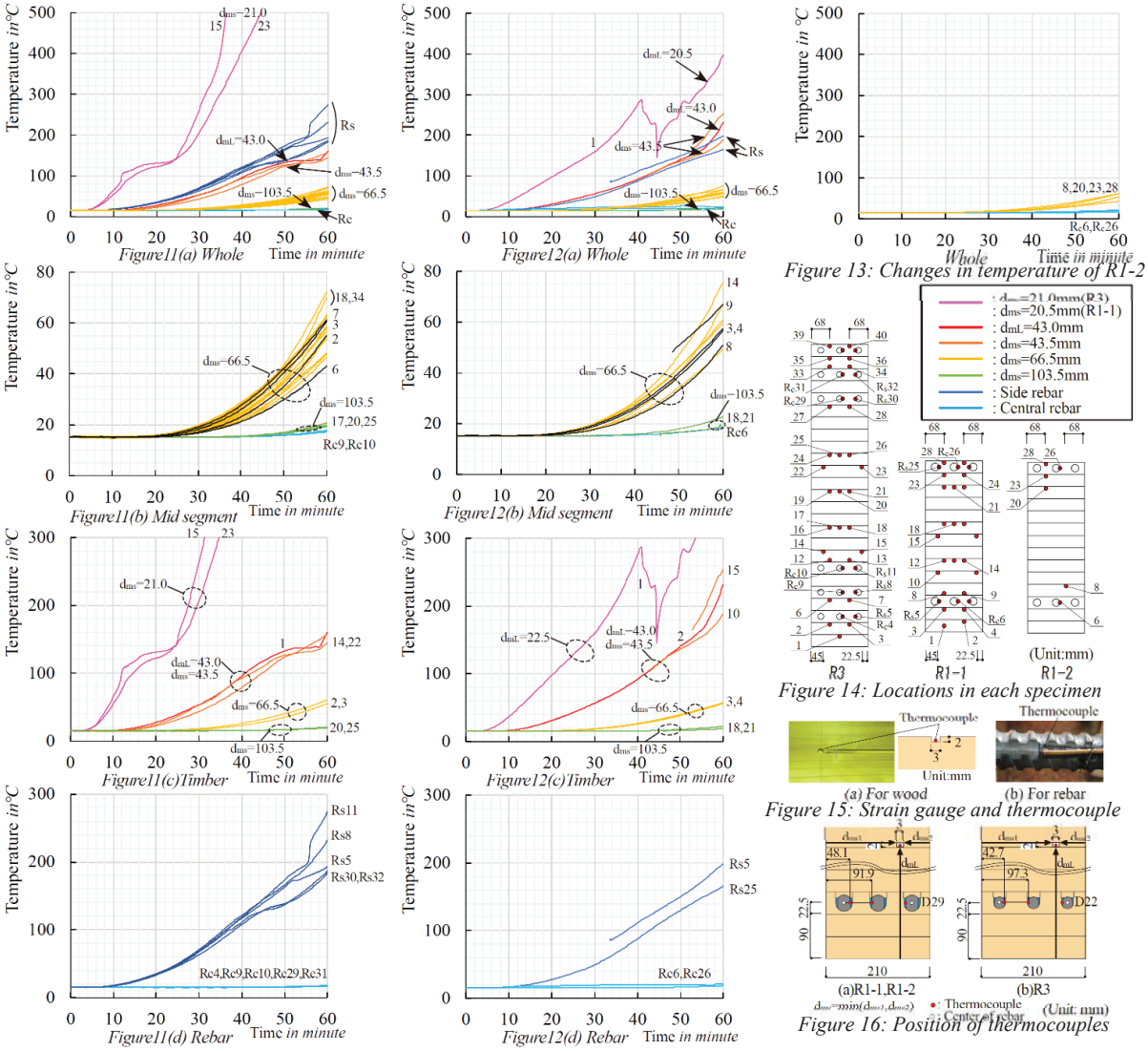

Figure 11: Changes in temperature of R3

Figure 12: Changes in temperature of R1-1

Figure 13: Changes in temperature of R1-2

Figure 14: Locations in each specimen

Figure 15: Strain gauge and thermocouple

Figure 16: Position of thermocouples

sudden increase as seen in R1-1 and R1-2. The third-layer array rebars had not yielded, therefor R3 is determined to have shear-failed just before bending yield. Figure 10 shows the axial strain profiles in the cross-section after the start of heating. Even after 60-minute of heating, the distribution can be to be approximately linear. Figure 10 shows the axial strain profiles in the cross-section after the start of heating. Even after 60 minutes of heating, the distribution can be to be approximately linear.

4.7 DAMAGE AFTER HEATING

Photo 4 shows cross-sections cut out form the specimens after the combustion test, from which their charred portion was removed. In R1-2 and R3, horizontal shear cracks occurred at the position surrounded by the yellow dotted curve. Boundary of charred portion is drawn in the Photo as red solid and broken curves. The blue curve indicates the boundary at 60-minute at a charring rate of 0.65 mm/minute in accordance with Eurocode 5, and the green curve indicates at the termination of additional loading (approximately 72 minutes). The boundary of the charred wood in R1-1 and R1-2 is consistent with the boundary calculated for both. On the other hand, charring of R3 progressed deeper than the calculated boundary. This is probably because R3 had a large span (L=9.4m), and its burning could not be suppressed by

https://doi.org/10.52202/080513-0710

spraying water from the side surface after 60-minute of heating.

4.8 CHANGE IN TEMPERATURE INSIDE BEAM DURING HEATING

4.8.1 Definition of symbols and terms

Figure 11-Figure 13 show temperature changes at the internal measurement points. Figure 11 is for R3; Figure 12 for R1-1, and Figure 13 for R1-2. Figure 14 shows measurement locations and numbers. The ● indicates the location of thermocouple. In R1-1, there were several locations where the thermocouple lead wire connection was incorrect and could not be measured. For those where the connection was corrected in time during heating, measurements were taken. The locations marked with numbers are the locations where measurements were possible. Figure 15 shows the installation of thermocouples in wood and on rebar. Figure 16 shows symbols for the depth of wood and locations of thermocouples on rebars.

4.8.2 Change of temperature in cross-section

Herein, the trend of the changes is described for R3, which has many measurement points. Temperature changes are shown in solid curves in Figure 11(a). The blue curves are for the side rebars, the light blue curves are for the central rebars, and the others are for the wood. At measuring points of 15 and 23 or Rs, the difference became larger when the temperature exceeded approximately 160℃, even if the depths of the side wood were the same. Figure 11(b) shows the temperature change of the central segment up to 80℃.; d_{ms}=66.5mm means the boundary of the central segment. There, the data for 20 locations are concentrated. The data for measuring points 2, 3, 6 and 7, which are close to the underside of the beam, are shown in black. The 20 locations have the same depth from the wood surface and are spread in beam height direction, but there are no effective differences in temperature change, corresponding to the height. The temperatures after 60-minute heating were 43-73℃. As wood is a natural material and is not strictly uniform, this suggests that some variation in the temperature data needs to be taken into account.

Points of d_{ms}=103.5mm is the center location of beam width, and green curve indicates the temperature of wood. Even at the end of the 60-minute heating, the temperature was 19.4-20.7℃, and the temperature rise was only 4.1-5.4℃. Because the temperature increase was very small, difference between the three locations was also small. Light blue curve is central rebar, and R_c9 and R_c10 are the minimum and maximum temperatures. The temperature rise of the central rebar is slightly slower after 50 minutes against the wood locations in the center of the width.

Figure 11(c) shows temperature changes at different depths of the wood up to 300℃.; d_{ms}=66.5mm is the boundary of the central segment, and d_{ms}=103.5mm is the location of the center of beam width, which shows the location that reached the maximum and minimum temperatures within each boundary during 60 minutes of heating, respectively. It is clear that the increase in temperature is suppressed as the depth of the wood increases. Measuring point 1 has d_{mL} of 43 mm, while measuring points 2 and 3 have d_{mL} of 88 mm. Temperatures at these points after 60-minutes of heating are 160.4℃, 55.1℃, and 60.6℃, respectively, and temperature of the central segment is suppressed to below 70℃, so it is clear that it is sufficient to bond a 90 mm lamina to the bottom of the beam. The measuring points 39 and 40 at the top of the beam are included in the curves of d_{ms}=66.5mm in Figure 11(b). The same trend was observed for R1-1 and R1-2.

5– SUMMARY

Loaded heating tests of three full-size beams were conducted to establish a 60-minute quasi-fireproofing design for steel bar-timber composite beam. The results are summarized as follows.

i: beam specimens were able to support the bending and shear strength capacities of the beams calculated using the proposed resistance portion section with 90mm-thickness lamina bonded to the bottom surface of beam. In addition, the load was increased immediately after the 60-minute heating, and the beam resisted up to 122-142% of the initially long-term load.

ii: From the strains of the steel bars and wood during heating and failures by additional loading after heating, the specimens have been classified into three categories: 1) one specimen whose strength capacity was determined by bending-yield, and the point of applied force failed after the curvature and deflection increased; 2) one specimen whose strength capacity was determined by bending-yield, and then shear failure occurred; 3) one specimen whose strength capacity was determined by shear failure.

iii: The beam was divided into three equal areas in beam width direction, and in the central segment, temperature of wood was suppressed to less than 70°C after 60 minutes of heating, and the rebar in the central segment was also suppressed to less than 30°C at

https://doi.org/10.52202/080513-0710

which the central rebar has exhibited resistance as normal steel.

iv: Both sides of the divided segments in the previous specimen reported in WCTE 2023 were charred, and side rebars there were bent during heating. However, the side rebars in this test, which were not anchored were not bent, extended axially, and loosely caught by the charred portion without falling off.

v: In the elastic range where load was introduced initially, the wood and rebar distorted as a complete, and even after 60 minutes of heating, the central segment within beam cross section was confirmed to have a strain distribution that allowed the assumption of the plane cross section after bending.

6–ACKNOWLEDGEMENT

This project was funded as Grants-in-Aid for Scientific Research ‘A’ by Japan Society for the Promotion of Science, 2022.

7– REFERENCES

[1] S. Shioya, et al.: An innovative hybrid timber structure in Japan: performance of column and beam, Wein, WCTE 2016

[2] S. Matsushita, S. Shioya: Burning test of steel bar - timber composite beam, Oslo, WCTE 2023.

[3] M. Nakamura, Y. Shimoirisa, S. Shioya: Steel bar - timber composite beam-column connection adopting steel damper, Brisbane, WCTE 2025.

[4] Eurocode 5, Design of timber structures - Part 1-2 General -Structural fire design, EN 1995-1-2, EUROPEAN COMMITTEE FOR STANDARD-IZATION, 2004